Preictal short-term plasticity induced by intracerebral 1 Hz stimulation

Olivier David [1 *] **, Agata WoÅºniak** [2 3] **, Lorella Minotti** [1 3] **, Philippe Kahane** [1 3 4]

[1] *GIN, Grenoble Institut des Neurosciences INSERM : U836 , CEA , Université Joseph Fourier - Grenoble I , CHU Grenoble , UJF - Site Santé La Tronche BP 170 38042 Grenoble Cedex 9,FR*

[2] *AGH University of Science and Technology , Cracow,PL*

[3] *LNPEE, Laboratoire de physiopathologie de l'épilepsie CHU Grenoble , 38043 Grenoble Cedex 9,FR*

[4] *CTRS-IDEE CHU Lyon , University Hospital, Lyon,FR*

* Correspondence should be adressed to: Olivier David <odavid@ujf-grenoble.fr >

Abstract

Short-term changes of intrinsic properties of neural networks play a critical role in brain dynamics. In that context, epilepsy is a typical pathology where the fast transition between interictal and ictal states is probably associated to intrinsic modifications of underlying networks. In this study, we focused on the correlates of plastic neural mechanisms in the intracerebral electroencephalogram (iEEG). Data were obtained during 1 Hz electrical stimulation in twenty patients suffering from temporal lobe epilepsy and implanted with intracerebral electrodes for clinical evaluation before resective surgery. First, we developed a procedure of analysis for localisation of the seizure onset zone based on brain excitability and plasticity defined as the average, and as the first-order (linear) modulation respectively, of the standard deviation of iEEG responses over stimulations. Our results suggest that the candidate epileptic focus is particularly prone to exhibiting short-term plasticity. Second, we used Dynamic Causal Modelling (DCM) to model explicitly short-term plasticity as a fast modulation of synaptic efficacies in either intrinsic or extrinsic connections to the focus. We found the two types of modulation both likely. Third, we used DCM to study the fast modulation of synaptic connectivity of long-range connections in neuronal networks restricted to the temporal lobe. Using DCM, we were able to estimate which structures expressed a strong modulatory input to the epileptic focus. Such early changes in interregional connectivity might be important for the initiation of electrically-induced seizures. They may also reflect some aspects of the pathogenesis of epilepsy in those patients.

MESH Keywords Adolescent ; Adult ; Algorithms ; Data Interpretation, Statistical ; Electric Stimulation ; Electrodes, Implanted ; Electroencephalography ; Epilepsy, Temporal Lobe ; physiopathology ; Female ; Humans ; Male ; Middle Aged ; Models, Statistical ; Nerve Net ; physiopathology ; Neuronal Plasticity ; physiology ; Seizures ; physiopathology ; Temporal Lobe ; physiopathology

Introduction

Short-term changes of intrinsic properties of neural networks play a critical role in brain dynamics (David et al., 2006b ; Zucker and Regehr, 2002). In cognitive neuroscience, the different shape of brain responses corresponding to different experimental conditions may be associated to fast modifications of connectivity between different responses (David et al., 2006a ; Kiebel et al., 2006). In clinical neuroscience, a typical disease related to brain plasticity is epilepsy where the fast transition between interictal (between epileptic seizures) and ictal (epileptic seizures, i.e. paroxysmal electro-clinical events) states is probably associated to intrinsic modifications of underlying networks. However, except when averaging evoked responses between experimental conditions, short-term plasticity is not usually modelled explicitly in human electrophysiology. It suggests that the importance of this brain mechanism may not be fully appreciated when analysing electroencephalographic (EEG) and magnetoencephalographic (MEG) signals.

In this study, we focus on the intracerebral EEG (iEEG) correlates of plastic neural mechanisms. Using the same data set obtained during 1 Hz electrical neurostimulation in patients suffering from temporal lobe epilepsy, our goal is to show how plasticity in iEEG responses can be modelled by adopting different levels of analysis. As a first approach, plasticity can be defined as the modification of the shape of successive induced responses to a particular stimulation. An implicit assumption is that plasticity is merely expressed at the synaptic level as changes in neural couplings. As a second approach, we show how synaptic plasticity can be explicitly modelled using generative models of iEEG (David et al., 2005 ; Rennie et al., 2002 ; Wendling et al., 2001). We use Dynamic Causal Modelling (DCM) (David et al., 2006a ; Kiebel et al., 2006) which consists in (i) assuming several neural networks with some connections expressing synaptic plasticity via a modulation of their strength between several conditions, (ii) estimating their parameters (intrinsic neural parameters and coupling between regions) from measured induced responses, (iii) comparing the different networks using Bayesian model selection to identify the most plausible functional hypothesis to explain the measured data (Penny et al., 2004).

A cortical imbalance between excitation and inhibition is likely to trigger abnormal electrical activity measured in iEEG and, thus, to be the pathophysiological basis for human partial epilepsy. In particular, repeated electrical stimulation of the cortex may induce transient modifications of neural network properties which can lead to the occurrence of epileptic events in patients (Chauvel et al., 1993 ; Kalitzin et al., 2005 ; Schulz et al., 1997 ; Valentin et al., 2002 ; Wilson et al., 1998). Although useful, neurostimulation for epilepsy evaluation is

not a usual clinical practice because it is invasive and complex. Only large centres fully equipped do perform this clinical exam as part of invasive recordings for presurgical evaluation following different protocols. These protocols include single pulse (Valentin et al., 2002 ; Valentin et al., 2005b ; Valentin et al., 2005a), paired pulse (Wilson et al., 1998), and repetitive (i.e. trains of stimuli, usually at frequencies comprised between 1 and 50 Hz) (Buser and Bancaud, 1983 ; Kahane et al., 1993 ; Kahane et al., 2004 ; Kalitzin et al., 2005) stimulation. They have been used particularly to localise the seizure onset zone (SOZ) in patients suffering from various forms of focal epilepsy. In clinical practice, when intracerebral stimulation is used, localisation of the SOZ is mostly based on the visual detection of pathological brain excitability during trains of stimuli (Kahane et al., 2004).

In this study, we describe a methodological approach to short-term plasticity of 1 Hz stimulation-induced evoked responses measured using intracranial electrodes in implanted patients. First, we develop an automatic procedure of analysis for standard localisation of the seizure onset zone based on brain excitability and plasticity. Second, we use DCM to model explicitly short-term plasticity as a modulation of synaptic strength. We first adopt a local DCM approach by focusing on the putative epileptic focus. In a subsequent DCM approach at a global level, we estimate the modulation of connectivity in networks distributed in the temporal lobe when a temporal structure is stimulated repetitively.

Materials and Methods

Experimental protocol

Patients included in this study have been selected for resective surgery and have undergone the standard presurgical evaluations clinical exams (high resolution MRI, video-EEG monitoring, neuropsychological testing). In addition, stereotaxic intracerebral EEG (SEEG) recordings were judged necessary before surgery to better delineate the brain areas to be resected. They were conducted according to a methodology described in (Kahane et al., 2004) which included 1 Hz intracerebral stimulation. This stimulation protocol is part of SEEG investigation at the Grenoble University Hospital for more than fifteen years (Kahane et al., 1993 ; Kahane et al., 2004). Fifty Hz stimulation is more classically used in other epilepsy centres, although there is no gold standard. Fifty Hz stimulation does not allow to easily observe brain responses online in a clinical environment, whereas this is the case for 1 Hz stimulation. This is the main reason why 1 Hz stimulation is also applied in our centre.

Patients were fully informed and gave their consent before being implanted and stimulated. Eleven to fifteen semirigid intracerebral electrodes were implanted per patient, either unilaterally (n=16) or bilaterally (n=4), in various cortical areas depending on the suspected origin of seizures. Each electrode was 0.8 mm in diameter and included 5, 10, 15 or 18 leads 2 mm in length, 1.5 mm apart (Dixi, Besanç on, France), depending on the target region. A preoperative stereotaxic magnetic resonance imaging and a stereotaxic teleradiography matched with Talairach and Tournoux's stereotaxic atlas (Talairach and Tournoux, 1988) were used to assess anatomical targets. Implantation of the electrodes was performed in the same stereotaxic conditions, with the help of a computer-driven robot. The location of the electrode contacts was subsequently reported on a stereotaxic scheme for each patient and defined by their coordinates in relation to the anterior commissure/posterior commissure plane.

Intracerebral recordings were performed using an audio-video-EEG monitoring system (Micromed, Treviso, Italy) that allowed to record simultaneously up to 128 contacts, so that a large range of mesial and cortical areas were sampled. Stimulation at 1 Hz (pulse width 3 milliseconds) was applied between two contiguous contacts at different levels along the axis of each electrode. The goals of the stimulation were the reproduction of the aura, the induction of an electroclinical seizure, and/or the localisation of an eloquent cortical area that has to be spared during surgery. Bipolar stimuli were delivered using a constant current rectangular pulse generator designed for a safe diagnostic stimulation of the human brain (Micromed, Treviso, Italy), according to parameters proved to produce no structural damage. The intensity used was 3 mA or less, depending on the stimulated site. Stimulation lasted 40 seconds or less (minimum: 8 seconds), depending on the type of the induced clinical response. When stimulation lasted less than 40 seconds, stimulation was stopped by the neurologist doing the experiment (L.M., P.K.) when fast synchronising discharges (low-voltage fast activity or activity recruiting fast discharges of spikes, (Kahane et al., 2006)) were observed. Low current stimulation (1 mA) was first performed and current was gradually increased (up to 3 mA, with an increment of 0.2 mA) if no effect was perceived. Seizures included in this study were induced using 3 mA. All bipolar derivations located in the cortex (and not in the white matter) were tested successively to find regions capable to initiate seizures.

Patients

We selected 20 patients (8 males, 12 females, aged from 18 to 51 years), who suffered from right (n=9) and left (n=11) temporal lobe epilepsy and in whom 1 Hz electrical stimulation had elicited at least one electroclinical seizure identical to those spontaneously recorded. Two seizures were induced in seven patients and four seizures in one patient. Detailed information about patients can be found in Table 1 .

Visual identification of the seizure onset zone

Electrically-induced seizures were inspected visually by clinicians (L.M., P.K.) to determine the site(s) of seizure onset and the exact timing of the first relevant electrical changes that occurred prior to the clinical onset of the seizure. Were considered as relevant the following iEEG patterns (Kahane et al., 2004): (i) low-voltage fast activity over 20 Hz; (ii) recruiting fast discharge (around 10 Hz or more) of spikes or polyspikes; (iii) rhythmic activity (around 10Hz) of low amplitude. The resulting ensemble of electrodes will be referred to as “Seizure Onset Zone” (SOZ) in the remaining of the study. Note that the sites of stimulation eliciting a seizure did not necessarily belong to the SOZ (see Table 1).

Analysis of EEG responses for identification of the seizure onset zone

EEG data were processed using an in-house developed toolbox of Statistical Parametric Mapping 5 (SPM5) software (www.fil.ion.ucl.ac.uk/spm , Wellcome Department of Imaging Neuroscience, University College London, UK) for dynamical analysis of iEEG. Electrode contacts were identified on each individual stereotaxic scheme, anatomically localised, and then reported in stereotaxic coordinates using Talairach and Tournoux’s proportional atlas (Talairach and Tournoux, 1988). Bipolar derivations were taken between adjacent electrode contacts (from 55 up to 114, depending on patients). Data were sampled at or down-sampled to 256 Hz (data in some patients were acquired at 512 Hz) and band-pass filtered between 0.8 and 40 Hz. To consider preictal activity only, stimulations performed after seizure onset were removed from any data analysis. Note that a seizure, once it has started, is not or very little influenced in the focus by subsequent stimulations (see Figures 2 –3 below or Figure 2 in online Supplementary Materials).

Brain excitability E, i.e. responsiveness to stimulations of a given brain region, was assumed to be reflected into the standard deviation of evoked responses averaged over stimulations:

$$E_i = \max_{win}\left(\frac{std(y_i^{1\dots N}(win))}{std(y_i^{baseline})}\right)$$

where win was a set of 45 time windows lined-up with the stimulations, comprised in the [0;1] second interval, of duration varying from 200 ms to 1 s (with 100 ms step) and with different offsets (from 0 to 800 ms with 100 ms step). Several time windows were used to take into account the various shapes of evoked responses. std denotes the standard deviation. N is the number of stimulations before seizure onset. y_i^n is the evoked response to stimulation n at channel i , $y_i^{1\dots N}$ is the concatenation of the evoked responses to the N stimulations. $y_i^{baseline}$ is baseline iEEG recorded during a 20 second period just prior to the first stimulation. The excitability E is a normalised measure, i.e. it is close to 1 when the stimulation has no particular effect, greater than 1 when evoked responses can be measured, and lower than 1 when ongoing EEG is suppressed. We used the standard deviation instead of the power to quantify the responsiveness of evoked responses because we found it was more robust to artefacts or to other confounds such as low-frequency drift. As a consequence, Eq. 1 defines brain excitability as the increase of EEG deviations from the mean induced by the stimulation, which is very similar to the common acceptation of the term “excitability” used in electrophysiology.

Short-term plasticity P was assumed to correspond to first-order changes over stimulations of the standard deviation of evoked responses. It was obtained by linear regression:

$$P_i = \max_{win,\,n}\left(\left|\frac{\beta_i^{win,\,n}(1)}{\beta_i^{win,\,n}(2)}\right|\right)$$

where $\beta_i^{win,n} = (XX^T)^{-1}XS_i^{win,n}$, $S_i^{win,n} = [std(y_i^{n\dots n+m}(win)),\ \dots,\ std(y_i^{m\dots n+m}(win))]^T$, $X = \begin{bmatrix} 1/m & 2/m & \dots & 1 \\ 1 & 1 & \dots & 1 \end{bmatrix}$. n varies from 0 to N-m. In the Results section, m was set to 10 or was equal to N if N< 10. P roughly expresses the percentage change of evoked responses standard deviation in a period of m stimulations (for instance, in the case of an increase of evoked responses due to plasticity, P =1 corresponds to a doubling of the strength of evoked responses – increase of 100% – between the beginning and the end of the window of interest).

Electrodes localising the epileptic focus were obtained by applying simultaneously a threshold T_E to the excitability E and a threshold T_P to the short-term plasticity P. The localisation accuracy was quantified as the minimal distance between selected electrodes by these thresholds and the visually pre-defined SOZ. The minimal distance from the electrodes belonging to the SOZ was computed for each electrode selected by the thresholds and averaged over all threshold-selected electrodes.

Dynamic causal modelling

Theory

DCM (David et al, 2006a ; Friston et al, 2003 ; Kiebel et al, 2006 ; Kiebel et al, 2007) explains brain responses to stimuli using biophysical models. This allows to rephrase observed differences in the shape of responses in terms of context-dependent coupling. The original generative model of DCM for EEG (David et al, 2005) combines the Jansen model (Jansen and Rit, 1995), a neural mass model originally developed for explaining visual responses, with rules of cortical-cortical connectivity derived from the analysis of connections

between the different cortical layers in the visual cortex of monkey (Crick and Koch, 1998). The resultant model (David et al, 2005) is a set of differential equations describing interactions between different inhibitory and excitatory neuronal populations, which can be easily manipulated to embed any hierarchical cortical-cortical network (see Figure 1 in online Supplementary Materials).

Because DCMs are biologically grounded, parameter estimation is constrained within a Bayesian framework and inferences about particular connections are made using their posterior or conditional density. The full set of equations for DCM specification and Bayesian parameter estimation can be found in the original papers (David et al, 2005 ; David et al, 2006a ; Friston et al, 2003 ; Kiebel et al, 2006 ; Penny et al, 2004). We just summarise below the most important steps.

A DCM is specified in terms of a state equation and an output equation:

$$\dot{x} = f(x, u, \theta)$$
$$y = g(x, \theta)$$

where y are measured data, x are the neuronal states, u are the extrinsic inputs and θ are the model parameters (inhibitory and excitatory synaptic time constants and efficacies, intrinsic and extrinsic connectivity, propagation delay). Functions f and g explain the measured dynamics. In standard DCM for EEG (David et al, 2006a ; Kiebel et al, 2006), y are a few principal modes of the scalp data and the function g is the head model used for source localisation. Here, because iEEG signals (y) are assumed to be a fair measure of the local depolarisation of principal cells (x), the function g is a simple one-to-one linear regression between x and y . Put simply, we assume there is no source localisation issue in iEEG bipolar recordings.

The main interest of DCM is to test for competing functional hypotheses. For each functional hypothesis, a model m is specified in terms of anatomical connections between regions and of the modulation of some connections by the experimental context. This is equivalent to constructing a specific function f (Eq. 3) for each model. After the estimation of parameters of each competing model, the models are compared to find the most likely model, or functional hypothesis. This can be done using Bayesian model selection where the evidence of each model, computed from estimated parameter distributions, is used to quantify the model plausibility (Penny et al, 2004). The most likely model is the one with the largest evidence. The evidence can be decomposed into two components: an accuracy term, which quantifies the data fit, and a complexity term, which penalises models with a large number of parameters. Therefore, the evidence embodies the two conflicting requirements of a good model, that it explains the data and is as simple as possible. Assuming each data set is independent of the others, the evidence at the group level (multi-subject analysis) is obtained by multiplying the marginal likelihoods or equivalently, by adding the log-evidences from each subject (Garrido et al., 2007). Note that the evidence can only be approximated under some assumptions. A possibility is to use the Akaike Information Criterion (AIC) or the Bayesian Information Criterion (BIC) (Penny et al., 2004) to get two estimates of the evidence and to decide for a significant plausibility of one model if the inference obtained with AIC and BIC assumptions is concordant. In the case AIC and BIC did not agree, we have used the BIC log-evidence to make a decision, if needed, because it is the most penalising criterion for complex models.

Functional hypotheses

The role of intrinsic and extrinsic connections

Because the candidate focus was not usually the stimulated region, it is important to evaluate whether the observed plasticity in the epileptic focus is due to the modulation of neural connections restricted to this region (intrinsic connections) or whether it is due to a modulation of the strength of afferent connections from surrounding networks (extrinsic connections). Using Bayesian model comparison, we will test these competing hypotheses (Figure 1). In the extrinsic model , we allow a variation of extrinsic inputs, keeping constant intrinsic efficacies. In the intrinsic model , we allow changes in intrinsic excitatory efficacies, keeping constant extrinsic inputs. In our models, extrinsic inputs are gamma functions which are parameterised by three parameters (amplitude, width and delay). Therefore, the modulation of N responses are particularly explained by 3*N parameters for the extrinsic hypothesis, whereas only N parameters (the N excitatory efficacies) are needed by the intrinsic hypothesis. This implies that, for an equivalent data fit, the model comparison will favour intrinsic models.

The network hypothesis

Assuming that extrinsic connections have an important role, we modelled them using distributed neural networks composed of four regions of the temporal lobe (five regions were modelled in a patient shown in online Supplementary Materials). We allowed the connectivity between regions to vary in order to model the changes of evoked responses observed between stimulations. This approach is complex and requires several assumptions to make it practically feasible which are described in the next section.

Data analysis

Data preprocessing

Typical evoked responses to 1 Hz neurostimulation can roughly be decomposed into a fast component in the first 150 ms after the stimulation and a late component (around 1–2 Hz). For the DCM analysis, we focused on early components only. To isolate early components, we bandpass-filtered the data between 5 and 40 Hz and select the first 150 ms following each stimulation (see online Supplementary Materials for further discussion on DCM data preprocessing).

Prior values of model parameters

As a first intracranial DCM study, we have chosen to make as few modifications as possible from the standard DCM for EEG (David et al., 2006a). To fit fast responses, we changed the DCM prior expectation of two sets of parameters: (i) excitatory and inhibitory fast time constants were set to 4 ms (instead of the standard 10 ms), (ii) propagation delays were set to 1 ms (instead of the standard 5 ms) because studied structures were close to each other. Otherwise, we took standard prior values (David et al., 2006a).

Patient selection, network architecture and searching procedure to test the network hypothesis

Testing the network hypothesis required to record activity in the stimulated region to allow the reconstruction of information transfer from the stimulated site to other parts of the network. Four contacts in the same region (two for stimulation, two for recording) were thus needed, which is not common to obtain due to the respective size of the electrode leads and of the structures explored. We were able to select only four patients (Patients 2, 7, 13 and 19) who met this important requirement.

Acknowledging the restricted neurophysiological plausibility of the DCM neural mass model for the different temporal structures, the distinction between forward, backward and lateral connections which is based on the distinction of the connection pattern between cortical layers was not tenable. Therefore, we have chosen to assume that all connections used in tested models were lateral. Lateral connections are symmetrical, which implies in neurodynamical terms that, if two regions are strongly bidirectionally coupled, they will oscillate with the same phase. If the coupling is asymmetrical, then the driving region can be easily differentiated from the driven region based on temporal precedence analysis.

The neurostimulation was modelled with a single extrinsic input to the region which was stimulated. Assuming (i) that all regions were connected in some direct or indirect way to the stimulated region, and (ii) that all possible connections were lateral and could express a short-term plasticity (i.e. were modulated through time), we calculated that 2432 models, in models composed of four regions, were possible candidates. Those models differ by their topology (existing connections between regions) assumed a priori . Given that it took approximately 2 hours to estimate the parameters of each model, it was obviously not possible to test every model. Thus, an alternative searching procedure was designed to converge quickly towards what could be the most plausible model:

- Step 1:
- Initialisation: Create the model with connections from the stimulated region to all other regions. Estimate parameters and compute the model evidence. Initialise the best model with this model.
- Step 2:
- Step 2.1: Identify the connections possible to add (in one step).
- Step 2.2: Loop on these connections and, for each added connections, compute the model evidence.
- Step 2.3: If a better model was found in Step 2.2, update the best model and go to Step 2. Otherwise go to Step 3.
- Step 3:
- Step 3.1: Identify the connections possible to remove (in one step).
- Step 3.2: Loop on these connections and, for each removed connections, compute the model evidence.
- Step 3.3: If a better model was found in Step 3.2, update the best model and go to Step 2.

Following this procedure, about 40 models were tested for each train of stimulations. Also, to save computational time, the searching procedure was performed on a data set composed only of the three first stimulations averaged together and of the three last (before seizure onset) stimulations averaged together. Then the parameters of the best model which was identified by the searching procedure were re-estimated using the full data set with all preictal stimulations.

Results

Data description

A prerequisite to 1 Hz electrical stimulation in the clinical setup at the Grenoble University Hospital is to induce seizures that resemble to spontaneous ones (Figure 2). This is particularly important to define those structures that are of low excitability threshold and may participate to the epileptogenic network. Only induced seizures exhibiting such an electro-clinical similarity were selected for further analysis of preictal evoked responses to stimulation.

Preictal evoked responses are only seen in brain regions thought to be either directly or indirectly connected to the site of stimulation. They are considered as physiological responses rather than closely related to some epileptic property of induced neural networks (Valentin et al., 2002). The number of components in evoked responses varied between recording sites and between patients. This is probably due to different patterns of connection where re-entrant loops do not have exactly the same effects on measured dynamics. The other observed phenomenon is the slow modulation of evoked responses over stimulation (Figure 3). We were able to distinguish a potentiation of evoked responses in most patients (18/20) and a depression of evoked responses in two patients only (Patients 4 and 6). We found no correlation between the type of response modulation and/or the stimulation sites, the recording sites, the underlying pathology, the postoperative outcome described in Table 1 .

Seizure onset localisation

Figure 4 summarises the results about the SOZ localisation based on excitability and plasticity of stimulation-induced responses. For given values of thresholds T_E and T_P , three variables were used: (left) The sensitivity , which is the probability over patients that at least one electrode was selected; (middle) The localisation accuracy , which is the average over patients and selected electrodes of the minimal distance between each selected electrodes and the SOZ; (right) The average over patients of the number of electrodes used to localise the seizure onset region .

Under the assumption that a sensitivity of 0.9 is the minimal acceptable sensitivity for an automatic procedure of epileptic focus detection (white border in Figure 4), the green asterisk indicates the optimal T_E value (T_E =6.8) when no information about plasticity is taken into account. On average, the localisation accuracy is then equal to 7.8 mm and 4.1 electrode contacts are used for SOZ localisation. As a comparison, the SOZ was visually defined with 4.7 electrode contacts on average. The magenta asterisk indicates optimal threshold values when information about both excitability and plasticity is used (T_E =5.75; T_P =5.05). Then the localisation accuracy decreases to 4.4 mm and only 3.7 electrode contacts are used on average.

The best localisation accuracy on average was 2.3 mm (T_E =8.475; T_P =5.225, white asterisk in Figure 4) using only 2.4 electrode contacts. This corresponds to strong effects in both excitability and plasticity. However, the specificity with such parameters was equal to 0.73 only (because of multiple induced seizures in some patients, SOZ localisation was in fact successful in 17/20=85% of patients with these thresholds). The results of SOZ localisation with these optimal parameters are detailed in Table 2 . It appears that there is no overlap between the SOZ defined visually and automatically in only one patient (Patient 5: amygdala versus anterior hippocampus). Otherwise the automatic procedure usually highlights a small subset of what can be defined visually.

These results highly suggest that at least a part of the seizure onset zone is particularly prone to exhibit short-term plasticity during preictal 1 Hz stimulation. We will now investigate this phenomenon further using DCM.

Dynamic Causal Modelling: The role of intrinsic and extrinsic connections

DCM showed a good ability to fit the data as illustrated in Figure 5 with examples of recorded (grey curves) and adjusted (black curves) time series in two patients (Patient 8/Seizure 1 and Patient 18). According to the log-evidence obtained using AIC and BIC assumptions (Figure 6), six patients showed evidence for a modulation on intrinsic excitation (Patients 4, 5, 8, 11, 12, 20) and seven showed evidence of a modulation of extrinsic connections (Patients 1, 2, 7, 9, 13, 15, 18). Remaining seven patients showed no consistent or non-reproducible (in the case of several seizures) evidences. For the group analysis, the log-evidence averaged over all available seizures (30) was not consistent between AIC and BIC (Figure 6 , right). As shown in Figure 5 , the difference between extrinsic and intrinsic hypotheses was small, suggesting either that intrinsic excitatory connections alone, or extrinsic excitatory inputs to the focus alone, are modulated. However, we did often observe that several regions were modulated together by focal stimulation. This speaks for a more complex connectivity analysis, elaborated in the next section.

Dynamic Causal Modelling: The network hypothesis

We present below the results obtained in the two patients stimulated in the amygdala (Patients 2 & 13). Patients 7 & 19, in whom seizures were induced twice, are discussed in the online Supplementary Materials.

Patient 2

This patient showed strong evoked responses in amygdala (Am, stimulated region), anterior hippocampus (AH, candidate focus), temporal pole (TP) and fusiform gyrus (FG). Those regions were included in the DCMs. Additional responses (weak and/or noisy) were found in the orbito-frontal cortex and insula. They were a priori excluded from the analysis. In the most plausible model (Figure 7), (i) Am sends projections to AH, TP and FG; (ii) AH is bidirectionnally coupled to Am and TP,; (iii) FG receives inputs from the Am and TP.

A progressive (between stimulations 1 and 20) increase of connectivity can be observed between Am and AH, in both directions. After stimulation 21, there is a large increase of connectivity from Am to AH and a decrease of connectivity from AH to Am. The connection between Am and AH appears thus critical in the preictal state. Am has also an impact on AH via TP since the connections from Am to TP and from TP to AH exhibit the same increase of connectivity as stimulations go along. The action of TP is enhanced by the recurrent loop formed by the feedback from AH onto TP. FG has a marginal role (receives inputs only and weak modulation of responses).

To sum up, the DCM analysis in this patient suggests a critical role of recurrent loops between AH/Am and between AH/TP. The repetitive stimulation of Am may have the property to initiate a short term potentiation of the excitatory outputs of Am towards AH and TP which extends to the entirety of the recurrent loops which connect AH to TP and Am.

Patient 13

The regions included in the DCMs of this patient were Am (stimulation site), AH (candidate focus), TP and middle temporal gyrus (T2). Additional weak responses were found in the anterior cingulate cortex and the insula and were a priori excluded from the analysis. Figure 8 shows the architecture of the most likely model: (i). Am sends projections to AH, TP and T2; (ii) AH receives inputs from AM via a relay in TP; (iii) T2 and TP are interconnected.

According to the strength of output connections, TP is the preferential target of Am, although the strength of that connection is reduced by repeated stimulations. The TP projections to T2 and AH are potentiated over stimulations and probably cause the observed dynamic changes in AH and T2. A weak suppression of TP responses due to a small decrease of the connection from Am to TP and from T2 to TP, is observed concomitantly with the potentiation of responses in AH and T2. Similarly to the previous patient, the estimated extrinsic inputs on Am are approximately constant over time, suggesting only weak intrinsic modulation of the amygdala excitability to neurostimulation.

To conclude, the DCM analysis suggests that, in this patient, repetitive stimulation of Am may induce a potentiation of projections of TP onto T2 and AH. The increase of inputs from TP to AH would be the main determinant to favour the emergence of paroxysmal dynamics in AH that may subsequently propagate to other brain regions.

Discussion

Intracerebral stimulation is a powerful approach for epilepsy evaluation during presurgical monitoring of patients (Buser and Bancaud, 1983 ; Chauvel et al., 1993 ; Kahane et al., 1993 ; Kahane et al., 2004 ; Kalitzin et al., 2005 ; Schulz et al., 1997 ; Valentin et al., 2002 ; Valentin et al., 2005b ; Valentin et al., 2005a ; Wilson et al., 1998). A significantly greater paired pulse suppression of population post-synaptic potentials was found on the epileptogenic side compared to the controlateral side in MLTE patients (Wilson et al., 1998). Using single pulse electrical stimulation, it has been suggested that epileptogenic regions, in either temporal or frontal lobe epilepsy, could exhibit more delayed response (up to 1 s) than other regions which show only early responses (<100 ms) (Valentin et al., 2002 ; Valentin et al., 2005b ; Valentin et al., 2005a). Using intermittent pulse stimulation in the 10–20 Hz frequency range, the spatial distribution of the excitability state in patients with TLE was found to be correlated with the most probable seizure onset zone (Kalitzin et al., 2005). In addition, and most importantly, the brain excitability was found to be the highest when seizure intervals were the shortest. This indicates that changes of excitability are a strong indicator of epileptogenic mechanisms.

Neurophysiological mechanisms underlying short-term plasticity in epileptic patients are best understood using in vitro experiments (Beck et al., 2000 ; Behr et al., 2001 ; Feng et al., 2003 ; Koch et al., 2005 ; Reichova and Sherman, 2004 ; Schmitz et al., 2001). In mesio-temporal lobe epilepsy (MTLE), paired-pulse induced changes of synaptic and intrinsic excitability are usually more easily observed in the hippocampus than in the neocortex (Koch et al., 2005). Systematically, modulation of NMDA or kainate receptors, depending on the structures involved, is found to be associated with electrically induced short-term plasticity in epilepsy. As shown by using trains of stimuli at different frequencies (Feng et al., 2003 ; Schiller and Bankirer, 2007), short-term plasticity is frequency-dependent and can be either inhibitory or excitatory. When repetitive stimulation has an anti-epileptic effect, this effect is mediated mainly by short-term synaptic depression of excitatory neurotransmission (Schiller and Bankirer, 2007). Analysing the different patterns of paired-pulse facilitation and paired-pulse inhibition may also give some insights for distinguishing neuronal drivers from neuronal modulators (Reichova and Sherman, 2004). In summary, in vitro experiments strongly suggest that repeated stimulations induce changes in neuronal properties that may be modelled and, possibly, estimated from iEEG signals in implanted patients.

In this study, we have first operationally evaluated 1 Hz intracerebral stimulation for the identification of epileptogenic regions. We have correlated the visually defined seizure onset zone with regions selected by the means of the average standard deviations of stimulation-induced responses (excitability) and of the linear trend of the standard deviations of those responses (short-term plasticity). As suggested by previous studies (Kalitzin et al., 2005 ; Schulz et al., 1997 ; Valentin et al., 2002 ; Valentin et al., 2005b ; Valentin et al., 2005a) and by more than a decade of clinical practice with this experimental protocol (Kahane et al., 2004), a strong correlation was found between regions which showed strong responses to stimulation and clinically identified seizure onset zones. We then showed that regions exhibiting slowly varying responses were even more correlated to the SOZ, in part because they were more focal, adding new evidence for the involvement of fast synaptic plasticity in epileptogenic mechanisms. In agreement with (Kalitzin et al., 2005), we found that short-term potentiation was correlated to seizure onset in most patients (18/20). Our results do not mean that it is clinically relevant to delineate more focal epileptogenic regions, but they point towards the fact that, in the pool of putative epileptic regions, a limited number show fast changes of the shape of responses induced by stimulation. Besides the localisation issue, searching for progressive modifications of neural responses to stimulations allows one to try to understand the transition between the interictal state and the ictal state. In that respect, further work is in progress to evaluate whether regions showing strong plasticity are correlated to regions exhibiting high frequency oscillations at seizure onset (Jirsch et al., 2006). Of course, our results rely on the assumption that the clinically defined (visually inspected) SOZ is a good marker of epileptogenic regions, which can be obviously a debatable issue (although used in clinical practice).

In contrast to in vitro studies, it is usually not possible to interact pharmacologically with the human brain in vivo to investigate neural mechanisms at the origins of the observed modulation of responses. Instead, we used a simple neural mass model to generate the iEEG signals of one or of several brain areas composed of inhibitory and excitatory neural populations (David et al., 2005). Our goal was to know whether the modulation of measured iEEG responses could be indeed thought of as a consequence of short-term plasticity of excitatory synaptic efficacies induced by repetitive stimulations. To do so, we have used DCM with two objectives: (i) to know whether it would be sufficient to assume that the modulation of synaptic efficacies is restricted to the putative focus or whether it would be expressed in other regions as well (extrinsic/intrinsic hypothesis); (ii) to study the connectivity in the temporal lobe and its short-term modulation during the preictal state of induced epileptic seizures (network hypothesis). In comparison to standard data driven approaches, DCM is unique because it proceeds to a connectivity analysis of macroscopic electrical data using neuronal models. Therefore, the estimated connectivity can be expressed directly in neuronal terms, i.e. synaptic efficacies, in contradistinction with other approaches based on correlation/synchronisation (David et al., 2004 ; Schindler et al., 2007) or multivariate autoregressive models (Baccala and Sameshima, 2001 ; Kaminski et al., 2001). This represents an important step forward a better understanding of brain functions.

For simplicity, we used the standard architecture of the neural mass model of DCM for EEG (David et al., 2006a ; Kiebel et al., 2006). This is a basic model of a cortical macro-column of the visual cortex (Jansen and Rit, 1995). Given that the cytoarchitecture of most structures in the temporal lobe does not conform to what can be found in the striate visual cortex, this model is certainly not the optimal neuronal model. However our objective was not to deal with a highly plausible neuronal model. Using the Jansen model as modified in (David et al., 2005) was simply a way to summarise the complex neuronal interactions in a neural mass model which has been shown to capture the basic dynamics of most types of EEG signals (David et al., 2004 ; David et al., 2005 ; David et al., 2006a ; David et al., 2006b ; David and Friston, 2003 ; Jansen and Rit, 1995 ; Kiebel et al., 2006 ; Wendling et al., 2000 ; Wendling et al., 2001). In fact, the departure from the proposed neuronal architecture of the true underlying neural networks was somewhat corrected for by the estimation of model parameters which adapts the dynamics generated by the model to the measured data. In addition, as we were most interested in the modulation of excitatory connections in a broad sense, the intrinsic architecture of brain regions was, to some extent, of no interest. More realistic models, i.e. with neural circuitry adapted to the different structures of the brain, would certainly be more convincing to study closely neural mechanisms that may be involved in specific regions or pathologies. However, development of specific models for temporal lobe epilepsy was out of the scope of this study. Future research is needed to evaluate the importance of refining the neural architecture of the models used in DCM.

After a group analysis including 30 seizures recorded in 20 patients, we did not find any evidence in favour of the two competing hypotheses about the role of extrinsic and intrinsic connections to the epileptic focus. It suggests first that observed short-term plasticity may be restricted to neural networks located in the epileptic focus. But it is equally plausible that the modulation of the shape of evoked responses may be due to the modulation of interregional connectivity. Given the fact that strong modulations were often observed simultaneously in multiple regions, we investigated further the hypothesis that the modulation is expressed at the level of connections between different regions belonging to the distributed network.

As an important selection criterion to test the network hypothesis, we imposed the stimulated structure to be also recorded, thereby restricting the analysis to four patients. Two patients were stimulated in amygdala (main text), one patient was stimulated twice in the fusiform gyrus (online Supplementary Materials), and the last patient was stimulated in the temporal pole and in the temporal neocortex T4 (online Supplementary Materials). By comparing the two patients stimulated in the amygdala (Patients 2 and 13), we will now discuss the reproducibility of DCM results between patients. Within-patient reproducibility is discussed in online Supplementary Materials using the

patient stimulated twice in the fusiform gyrus (Patient 19). Finally, the reproducibility of the effects of neurostimulation in regard to a change of the site of stimulation is discussed using the fourth patient (Patient 7) in online Supplementary Materials.

The two patients stimulated in the amygdala showed a strong increase of the amplitude of responses in the anterior hippocampus a few stimulations (five in Patient 2, three in Patient 13) before the seizure onset. In both patients, this corresponded to an increase of effective connectivity between the temporal pole and the anterior hippocampus (Figures 7 & 8). In Patient 2, the direct influence of the amygdala onto the anterior hippocampus was also increased (Figure 7). These connections are supported by anatomical studies (Chabardes et al., 2002): the hippocampus receives afferents from all over the anterior temporal cortex and an amygdalo-temporal fascicle which originates at the rostrolateral surface of the amygdala and specifically connects to the temporal pole has been described in human (Klingler and Gloor, 1960). Furthermore, it has been suggested from visual analysis of iEEG recordings that the temporal pole may be a determinant structure, concomitantly with the hippocampus, during the onset of seizures in temporal lobe epilepsy in many patients (Chabardes et al., 2005 ; Kahane et al., 2002). The results obtained from the DCM study in those two patients agree with this part of the literature. They also call for an interpretation of the genesis of a certain type of mesial temporal lobe epilepsy as a preictal increase of the hippocampal afferents coming from the temporal pole, which could be triggered by the amygdala. This putative type of mesial temporal lobe epilepsy remains to be fully characterised. Note that an increase of synaptic connectivity induces an increase of synchrony between distant regions. Such preictal synchronisation associated with a preictal increase of synaptic connectivity has been described between mesial structures (Bartolomei et al., 2004).

Conclusion

We have shown that a limited number of structures in temporal lobe epilepsy, identifiable to the candidate epileptic focus, is particularly prone to express fast changes in their responses to repetitive 1 Hz neurostimulation. In our small cohort of patients, we did not find any correlation between expressed plasticity and patients' pathologies. However, studying short-term plasticity may constitute an added value more easily exploitable in prospective studies than in retrospective studies such as ours. The signal analysis to identify changes in the shape or amplitude of responses induced by neurostimulation is rather straightforward and can be used in clinical routine. The biophysical description of short-term plasticity in epilepsy is much more difficult to perform, though extremely interesting to understand epileptogenic mechanisms. In particular, it is time-consuming because it implies nonlinear identification of complex dynamical systems. However such approach is still in its infancy and is likely to be developed further in the near future. For instance, an important issue is to better understand the intrinsic dynamics of short term plasticity: Why is it progressive? What is the meaning of apparent random fluctuations? Can it be used to infer more global dynamical features on neural networks? A first direction to answer to these questions, among other possibilities, has been proposed where the theory of autonomous systems has been combined to the formalism of DCM (David, 2007). Being able to deal with this sort of interrogations is a step forward in neuroimaging and electrophysiology data analysis that will allow new interpretations of clinical and physiological data in integrated neuroscience.

Ackowledgements:

This study was supported by Inserm and the Erasmus program (A.W.).

References:

- Baccala LA , Sameshima K . 2001 ; Partial directed coherence: a new concept in neural structure determination . Biol Cybern . 84 : 463 - 474
- Bartolomei F , Wendling F , Regis J , Gavaret M , Guye M , Chauvel P . 2004 ; Pre-ictal synchronicity in limbic networks of mesial temporal lobe epilepsy . Epilepsy Res . 61 : 89 - 104
- Beck H , Goussakov IV , Lie A , Helmstaedter C , Elger CE . 2000 ; Synaptic plasticity in the human dentate gyrus . J Neurosci . 20 : 7080 - 7086
- Behr J , Heinemann U , Mody I . 2001 ; Kindling induces transient NMDA receptor-mediated facilitation of high-frequency input in the rat dentate gyrus . J Neurophysiol . 85 : 2195 - 2202
- Buser P , Bancaud J . 1983 ; Unilateral connections between amygdala and hippocampus in man. A study of epileptic patients with depth electrodes . Electroencephalogr Clin Neurophysiol . 55 : 1 - 12
- Chabardes S , Kahane P , Minotti L , Hoffmann D , Benabid AL . 2002 ; Anatomy of the temporal pole region . Epileptic Disord . 4 : (Suppl 1) S9 - 15
- Chabardes S , Kahane P , Minotti L , Tassi L , Grand S , Hoffmann D , Benabid AL . 2005 ; The temporopolar cortex plays a pivotal role in temporal lobe seizures . Brain . 128 : 1818 - 1831
- Chauvel P , Landre E , Trottier S , Vignel JP , Biraben A , Devaux B , Bancaud J . 1993 ; Electrical stimulation with intracerebral electrodes to evoke seizures . Adv Neurol . 63 : 115 - 121
- Crick F , Koch C . 1998 ; Constraints on cortical and thalamic projections: the no-strong-loops hypothesis . Nature . 391 : 245 - 250
- David O . 2007 ; Dynamic causal models and autopoietic systems . Biol Res .
- David O , Cosmelli D , Friston KJ . 2004 ; Evaluation of different measures of functional connectivity using a neural mass model . Neuroimage . 21 : 659 - 673
- David O , Friston KJ . 2003 ; A neural mass model for MEG/EEG: coupling and neuronal dynamics . Neuroimage . 20 : 1743 - 1755
- David O , Harrison L , Friston KJ . 2005 ; Modelling event-related responses in the brain . Neuroimage . 25 : 756 - 770
- David O , Kiebel SJ , Harrison LM , Mattout J , Kilner JM , Friston KJ . 2006a ; Dynamic causal modeling of evoked responses in EEG and MEG . Neuroimage . 30 : 1255 - 1272
- David O , Kilner JM , Friston KJ . 2006b ; Mechanisms of evoked and induced responses in MEG/EEG . Neuroimage . 31 : 1580 - 1591
- Feng L , Molnar P , Nadler JV . 2003 ; Short-term frequency-dependent plasticity at recurrent mossy fiber synapses of the epileptic brain . J Neurosci . 23 : 5381 - 5390
- Friston KJ , Harrison L , Penny W . 2003 ; Dynamic causal modelling . Neuroimage . 19 : 1273 - 1302
- Garrido MI , Kilner JM , Kiebel SJ , Stephan KE , Friston KJ . 2007 ; Dynamic causal modelling of evoked potentials: A reproducibility study . Neuroimage .
- Jansen BH , Rit VG . 1995 ; Electroencephalogram and visual evoked potential generation in a mathematical model of coupled cortical columns . Biol Cybern . 73 : 357 - 366
- Jirsch JD , Urrestarazu E , LeVan P , Olivier A , Dubeau F , Gotman J . 2006 ; High-frequency oscillations during human focal seizures . Brain . 129 : 1593 - 1608

- Kahane P , Chabardes S , Minotti L , Hoffmann D , Benabid AL , Munari C . 2002 ; The role of the temporal pole in the genesis of temporal lobe seizures . Epileptic Disord . 4 : (Suppl 1) S51 - S58
- Kahane P , Landré E , Minotti L , Francione S , Ryvlin P . 2006 ; The Bancaud and Talairach view on the epileptogenic zone: a working hypothesis . Epileptic Disord . 8 : S16 - S35
- Kahane P , Minotti L , Hoffmann D , Lachaux J-P , Ryvlin P . Editor: Rosenow F , Lüders HO . 2004 ; Invasive EEG in the definition of the seizure onset zone: depth electrodes . Handbook of Clinical Neurophysiology . 3 : Elsevier BV ; Amsterdam 109 - 133
- Kahane P , Tassi L , Francione S , Hoffmann D , Lo RG , Munari C . 1993 ; Electroclinical manifestations elicited by intracerebral electric stimulation “shocks” in temporal lobe epilepsy . Neurophysiol Clin . 23 : 305 - 326
- Kalitzin S , Velis D , Suffczynski P , Parra J , da Silva FL . 2005 ; Electrical brain-stimulation paradigm for estimating the seizure onset site and the time to ictal transition in temporal lobe epilepsy . Clin Neurophysiol . 116 : 718 - 728
- Kaminski M , Ding M , Truccolo WA , Bressler SL . 2001 ; Evaluating causal relations in neural systems: granger causality, directed transfer function and statistical assessment of significance . Biol Cybern . 85 : 145 - 157
- Kiebel SJ , David O , Friston KJ . 2006 ; Dynamic causal modelling of evoked responses in EEG/MEG with lead field parameterization . Neuroimage . 30 : 1273 - 1284
- Kiebel SJ , Garrido MI , Friston KJ . 2007 ; Dynamic causal modelling of evoked responses: The role of intrinsic connections . Neuroimage . 36 : 332 - 345
- Klingler J , Gloor P . 1960 ; The connections of the amygdala and of the anterior temporal cortex in the human brain . J Comp Neurol . 115 : 333 - 369
- Koch UR , Musshoff U , Pannek HW , Ebner A , Wolf P , Speckmann EJ , Kohling R . 2005 ; Intrinsic excitability, synaptic potentials, and short-term plasticity in human epileptic neocortex . J Neurosci Res . 80 : 715 - 726
- Penny W , Stephan K , Mechelli A , Friston K . 2004 ; Comparing dynamic causal models . Neuroimage .
- Reichova I , Sherman SM . 2004 ; Somatosensory corticothalamic projections: distinguishing drivers from modulators . J Neurophysiol . 92 : 2185 - 2197
- Rennie CJ , Robinson PA , Wright JJ . 2002 ; Unified neurophysical model of EEG spectra and evoked potentials . Biol Cybern . 86 : 457 - 471
- Schiller Y , Bankirer Y . 2007 ; Cellular mechanisms underlying antiepileptic effects of low- and high-frequency electrical stimulation in acute epilepsy in neocortical brain slices in vitro . J Neurophysiol . 97 : 1887 - 1902
- Schindler K , Leung H , Elger CE , Lehnertz K . 2007 ; Assessing seizure dynamics by analysing the correlation structure of multichannel intracranial EEG . Brain . 130 : 65 - 77
- Schmitz D , Mellor J , Nicoll RA . 2001 ; Presynaptic kainate receptor mediation of frequency facilitation at hippocampal mossy fiber synapses . Science . 291 : 1972 - 1976
- Schulz R , Luders HO , Tuxhorn I , Ebner A , Holthausen H , Hoppe M , Noachtar S , Pannek H , May T , Wolf P . 1997 ; Localization of epileptic auras induced on stimulation by subdural electrodes . Epilepsia . 38 : 1321 - 1329
- Talairach J , Tournoux P . 1988 ; Co-planar stereotaxic atlas of the human brain . Thieme ; Stuttgart
- Valentin A , Alarcon G , Garcia-Seoane JJ , Lacruz ME , Nayak SD , Honavar M , Selway RP , Binnie CD , Polkey CE . 2005a ; Single-pulse electrical stimulation identifies epileptogenic frontal cortex in the human brain . Neurology . 65 : 426 - 435
- Valentin A , Alarcon G , Honavar M , Garcia Seoane JJ , Selway RP , Polkey CE , Binnie CD . 2005b ; Single pulse electrical stimulation for identification of structural abnormalities and prediction of seizure outcome after epilepsy surgery: a prospective study . Lancet Neurol . 4 : 718 - 726
- Valentin A , Anderson M , Alarcon G , Seoane JJ , Selway R , Binnie CD , Polkey CE . 2002 ; Responses to single pulse electrical stimulation identify epileptogenesis in the human brain in vivo . Brain . 125 : 1709 - 1718
- Wendling F , Bartolomei F , Bellanger JJ , Chauvel P . 2001 ; Interpretation of interdependencies in epileptic signals using a macroscopic physiological model of the EEG . Clin Neurophysiol . 112 : 1201 - 1218
- Wendling F , Bellanger JJ , Bartolomei F , Chauvel P . 2000 ; Relevance of nonlinear lumped-parameter models in the analysis of depth- EEG epileptic signals . Biol Cybern . 83 : 367 - 378
- Wilson CL , Khan SU , Engel J Jr , Isokawa M , Babb TL , Behnke EJ . 1998 ; Paired pulse suppression and facilitation in human epileptogenic hippocampal formation . Epilepsy Res . 31 : 211 - 230
- Zucker RS , Regehr WG . 2002 ; Short-term synaptic plasticity . Annu Rev Physiol . 64 : 355 - 405

Figure 1

Alternative DCMs of the epileptic focus tested to explain observed short term plasticity in this region. The bold arrows correspond to the modulated connections. In the extrinsic model, extrinsic input u is modulated. In the intrinsic model, intrinsic excitatory efficacy H_e varies. Note that the loop between excitation and inhibition captures the concept of interactions between excitatory and inhibitory neuronal populations but does not exactly reflect the architecture of the Jansen model (see Fig. 1 in online Supplementary Materials).

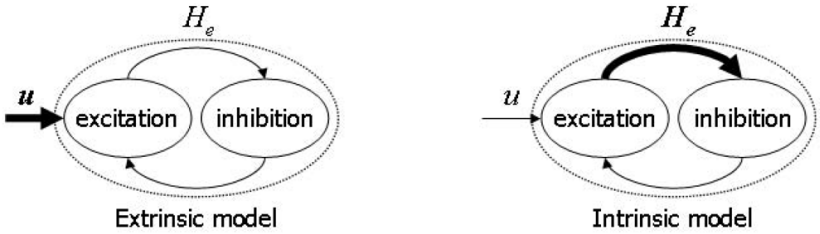

Figure 2

Intracerebral EEG recordings of a spontaneous seizure and of an induced seizure in the same patient (Patient 7). The induced seizure was obtained by 1 Hz stimulation on the top electrode (i'2-i'3: left temporal pole, flat signal during stimulation – no recording). The last five evoked responses to stimulation can be observed before the onset of the induced seizure indicated by the arrow. In both spontaneous and induced seizures, the onset is characterised by focal fast rhythms on the fifth electrode from top, followed a few seconds later by a diffusion to other electrodes where slow oscillations occur.

Figure 3

Different observed types of stimulation-induced modulation: a gradual increase of evoked responses (Patient 19, posterior hippocampus) and a gradual decrease of evoked responses (Patient 4, anterior hippocampus).

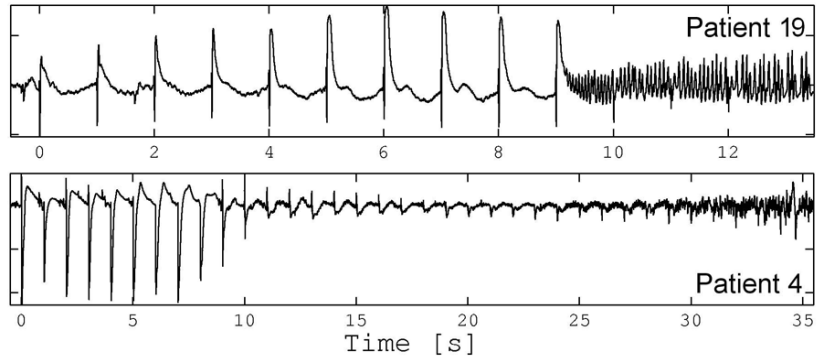

Figure 4

Seizure onset localisation as a function of excitability threshold T_E and plasticity threshold T_P . Green asterisk: optimal T_E value (T_E =6.8) when no information about plasticity is taken into account. Magenta asterisk: optimal threshold values (T_E =5.75; T_P =5.05) when information about both excitability and plasticity is used, with a sensitivity > 0.9 (white border). White asterisk: best localisation accuracy (T_E =8.475; T_P =5.225). See main text for more details.

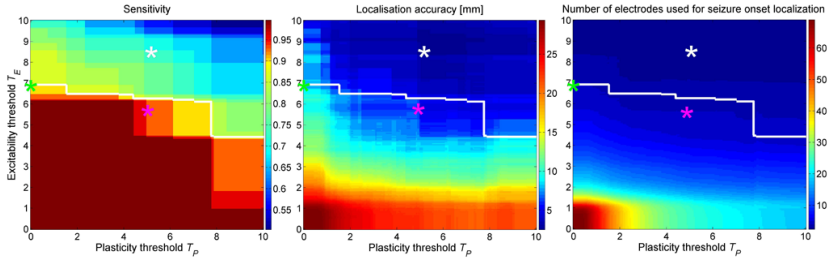

Figure 5

Neural modelling of short-term plasticity in the epileptic focus for two patients (left: Patient 8; right: Patient 18). Model time series (grey) are superimposed on the measured time series (black). The first row (Extrinsic) corresponds to the modulation of the extrinsic input u to the focus (gamma function with three parameters: amplitude, width and onset). The second row (Intrinsic) corresponds to the modulation of intrinsic excitatory efficacies H_e (one parameter). The time series of H_e and of the power of u are shown in the third row.

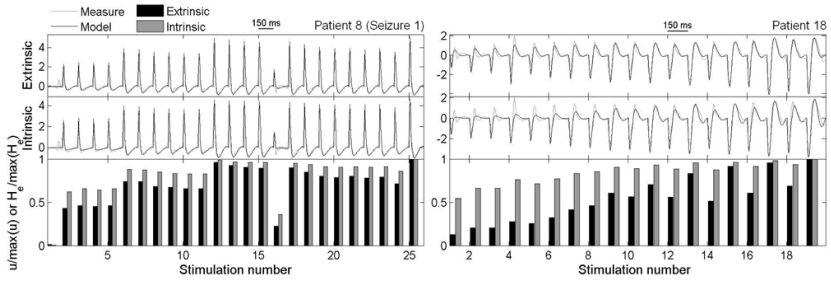

Figure 6

Model comparison for the role of the modulation of extrinsic and intrinsic excitatory connections. Left: The log-evidences for all seizures are shown (AIC and BIC assumptions). Right: Log-evidence for the group. BIC evidences are lower than AIC evidences because complexity of the models is more penalising.

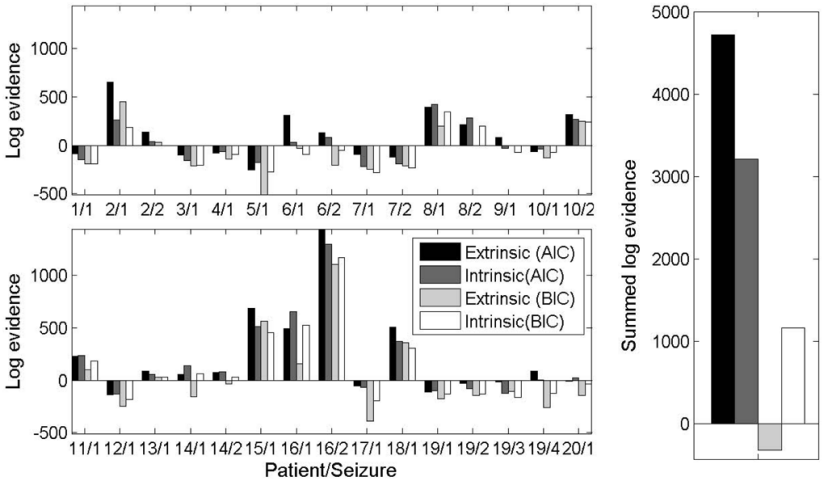

Figure 7

Most likely model estimated during the amygdala (Am) stimulation in Patient 2. Left: Topography of the estimated DCM superimposed on a schematic of the temporal lobe. The dark grey region indicates the candidate focus (AH: anterior hippocampus). FG: fusiform gyrus; TP: temporal pole. Each connection is associated with a time series of estimated effective connectivity (black bars) and a number in italic (slope) which indicates whether the connection strength is increased (positive slope) or decreased (negative slope) by repeated stimulations. The slope M_i^n of connection i at stimulation n was defined as $M_i^n = \boldsymbol{\beta}(1)$ where $\beta = (XX^T)^{-1} XS$, $S=[c_i^{1+n}, \ldots, c_i^{m+n}]^T, X=\begin{bmatrix}1 & m-0.5 & 2 & m-0.5 & \ldots & 0.5\\ 1 & & 1 & & \ldots & 1\end{bmatrix}$. C_i^n is the coupling strength of connection i at stimulation n. n varied from 0 to N-m. m was set to 10 or was equal to the total number of stimulations N if N <10. When computing the slopes, obvious outliers were removed to track only slow changes. Figure indicates the maximal value of M_i^n when n is varied. Broken arrows indicate connections inhibited by repetitive stimulation (slope<0). Thick arrows indicate connections strongly modulated (|slope|>1.5). Right: Measured (black) and adjusted (grey) time series, after normalisation of their variance.

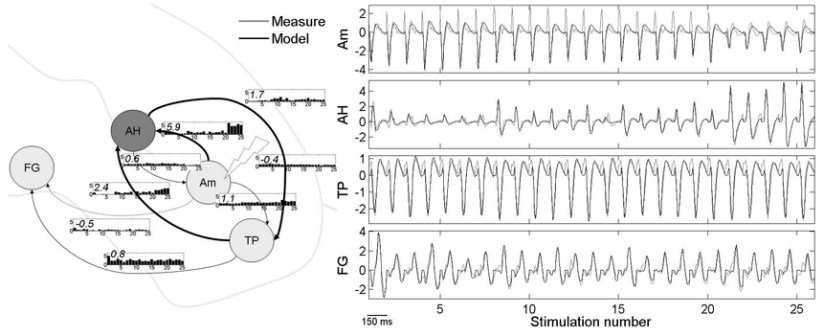

Figure 8

Most likely model estimated during the amygdala (Am) stimulation in Patient 13. Same format as in Figure 7 . AH: anterior hippocampus; T2: middle temporal gyrus; TP: temporal pole.

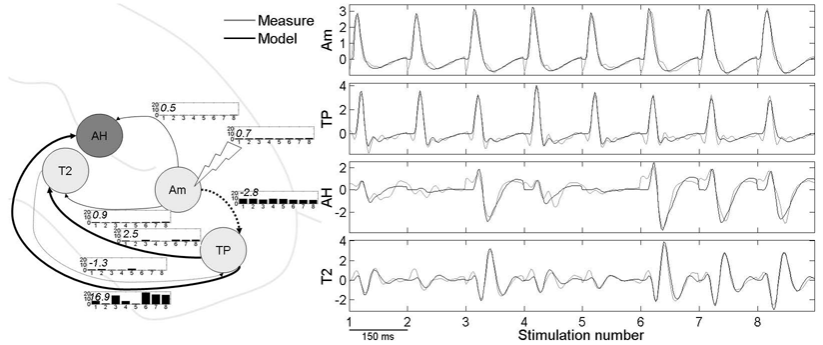

Table 1
Patient information

Patient	Sex	Age at SEEG	Past history	Epilepsy onset	MRI findings	Seizure side	Stimulation site	SOZ	Surgery	Post-op follow up	Outcome 1
1	F	40y 11m	meningitis	12 y	R HcS L T arachnoidian cyst	R	**ant Hc**	amyg, ant/post Hc, pHcG, T4	R T disconnection	4y 2m	IA
2	F	24y 7m	FS	2 y	L HcS	L	**amyg, post Hc**	ant/post Hc, basal T	L T disconnection	5y 3m	IIB
3	M	39y 11m	FS	2 y	L HcS	L	**ant Hc**	post Hc	L T lobectomy	2y 1m	IA
4	M	18y 1m	FS	15 y	L HcS L fronto-basal aspecific lesion	L	**pHcG**	ant/post Hc	L T disconnection + lesionnectomy	5y 3m	IA
5	F	36y	perinatal injury	4 y	R HcS	R	**ant Hc**	amyg	R T lobectomy	1y 7m	IIB
6	F	42 y	FS	4 y	R HcS	R	**amyg**	FG, ant Hc	R T lobectomy	6 m	IIIA
7	F	18 y	FS	6 y	L HcS	L	**T4, TP**	amyg, ant Hc, TP	L T lobectomy	18 m	IIC
8	F	38 y	FS	3 y	R HcS	R	**ant Hc**	amyg, ant Hc	R T lobectomy	8m	IA
9	F	41 y	FS	19 y	R HcS L sylvian arachnoidian cyst	R	**pHcG**	ant/post Hc	R T lobectomy	3 m	IA
10	M	34y 4m	FS	8 y	R HcS R hemispheric atrophy	R	**ant/post Hc**	ant/post Hc	R T disconnection	4y 8m	IA
11	F	27 y	–	7 y	L HcS	L	**ant Hc**	post Hc	L T lobectomy	1 y	IA
12	M	27 y	–	3 y	R HcS epiphyseal cyst	R	**pHcG**	amyg, ant Hc	R T lobectomy	11 m	IA
13	F	51 y	–	41 y	–	L	**amyg**	ant/post Hc, T2	L T lobectomy	2 m	IA
14	M	37y 5m	Head trauma	23 y	R T postero-basal posttraumatic scarr	R	**T4, ant Hc**	post Hc, pHcG, TP	R T lobectomy	4y 6m	IA
15	F	41y	FS	21 y	L HcS	L	**post Hc**	ant Hc, pHcG	L T lobectomy	1 m	IA
16	M	17y 8m	encephalitis	15y	L HcS L T atrophy	L	**ant Hc, pHcG**	amyg, ant Hc, pHcG	L T lobectomy	1y 8m	IA
17	M	41y 7m	–	10 y	R HcS pituitary adenoma	R	**ant Hc**	ant Hc	R T lobectomy	2y 4m	IA
18	M	18y 4m	FS	3y	R HcS R fronto-basal cavernoma	R	**ant Hc**	amyg, TP	R T disconnetion + lesionnectomy	5y 8m	IA
19	F	23y 4m	FS	9y	R HcS	R	**amyg, ant/post Hc**	FG, ant/post Hc	R T disconnection	5y 8m	IA
20	F	41 y	FS	7 y	L HcS	L	**post Hc**	ant Hc, pHcG	L T lobectomy	3 m	IA

1 According to Engel's Classification.
amyg: amygdala; ant/post: anterior/posterior; F: frontal; FG: fusiform gyrus; FS: febrile seizure; Hc: hippocampus; HcS: hippocampal sclerosis; m: month; pHcG: parahippocampal gyrus; R/L: right/left; T: temporal; TP: temporal pole; T2: middle temporal gyrus; T4: lateral temporal-occipital gyrus; y: year

Table 2

SOZ localization with optimized parameters (T_E =8.475; T_P =5.225, white asterisk in Figure 5).

Patient	SOZ	Selected regions by automatic EEG analysis	Localisation accuracy [mm]
1	amyg, ant/post Hc, pHcG, T4	post Hc	0
2	ant/post Hc, basal T	ant Hc	0
3	post Hc	post Hc	0
4	ant/post Hc	ant/post Hc	0
5	amyg	ant Hc	19.2
6	FG, ant Hc	FG, ant Hc, amyg	7.0
7	amyg, ant Hc, TP	amyg, ant Hc, insula, TP	5.7
8	amyg, ant Hc	amyg, ant Hc	4.7
9	ant/post Hc	post Hc	0
10	ant/post Hc	ant Hc	0
11	post Hc	post Hc	0
12	amyg, ant Hc	ant Hc	0
13	ant/post Hc, T2	ant Hc	0
14	post Hc, pHcG, TP	pHcG	0
15	ant Hc, pHcG	ant Hc	0
16	amyg, ant Hc, pHcG	ant Hc	0
17	ant Hc	ant Hc	0
18	amyg, TP	TP	0
19	FG, ant/post Hc	FG, ant/post Hc	2.1
20	ant Hc, pHcG	ant Hc	0

Same abbreviations as in Table 1 . No electrode contact was detected in patients indicated in italic with the thresholds specified. For these patients, the first electrode contact showing up when decreasing the most conservative threshold is indicated.